

# Accepted Manuscript

Green synthesis and photophysical properties of novel 1*H*-imidazo[4,5-*f*][1,10]phenanthroline derivatives with blue/cyan two-photon excited fluorescence

Yu-Lu Pan, Zhi-Bin Cai, Li Bai, Fei-Fei Ma, Sheng-Li Li, Yu-Peng Tian



PII: S0040-4020(17)30333-2

DOI: [10.1016/j.tet.2017.03.075](https://doi.org/10.1016/j.tet.2017.03.075)

Reference: TET 28581

To appear in: *Tetrahedron*

Received Date: 20 January 2017

Revised Date: 23 March 2017

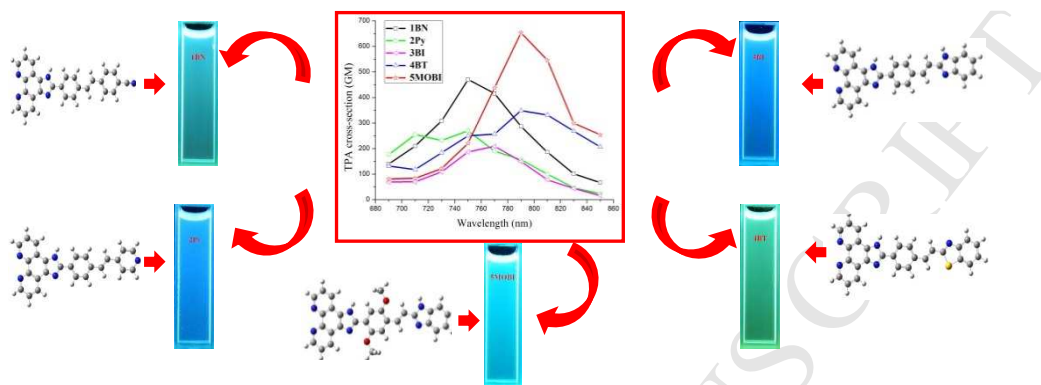
Accepted Date: 27 March 2017

Please cite this article as: Pan Y-L, Cai Z-B, Bai L, Ma F-F, Li S-L, Tian Y-P, Green synthesis and photophysical properties of novel 1*H*-imidazo[4,5-*f*][1,10]phenanthroline derivatives with blue/cyan two-photon excited fluorescence, *Tetrahedron* (2017), doi: 10.1016/j.tet.2017.03.075.

This is a PDF file of an unedited manuscript that has been accepted for publication. As a service to our customers we are providing this early version of the manuscript. The manuscript will undergo copyediting, typesetting, and review of the resulting proof before it is published in its final form. Please note that during the production process errors may be discovered which could affect the content, and all legal disclaimers that apply to the journal pertain.

**Graphical abstract**

A series of novel 1*H*-imidazo[4,5-*f*][1,10]phenanthroline derivatives were synthesized via the solvent-free Debus–Radziszewski reaction. They display both large two-photon absorption cross-sections and strong blue/cyan fluorescence.



**Green synthesis and photophysical properties of novel  
1*H*-imidazo[4,5-*f*][1,10]phenanthroline derivatives with blue/cyan  
two-photon excited fluorescence**

Yu-Lu Pan <sup>a</sup>, Zhi-Bin Cai <sup>a,\*</sup>, Li Bai <sup>a</sup>, Fei-Fei Ma <sup>a</sup>, Sheng-Li Li <sup>b</sup>, Yu-Peng Tian <sup>b</sup>

<sup>a</sup> *College of Chemical Engineering, Zhejiang University of Technology, Hangzhou 310014, PR China*

<sup>b</sup> *Department of Chemistry, Anhui Province Key Laboratory of Functional Inorganic Materials, Anhui University, Hefei 230039, PR China*

**Abstract**

A simple, rapid, and highly efficient method has been developed for the synthesis of a series of novel 1*H*-imidazo[4,5-*f*][1,10]phenanthroline derivatives (**1BN**, **2Py**, **3BI**, **4BT**, and **5MOBI**) via a three-component, one-pot reaction under solvent-free conditions. Their structures were characterized by FT-IR, <sup>1</sup>H NMR, <sup>13</sup>C NMR, MS, and elemental analysis. Their photophysical properties, including linear absorption, one-photon excited fluorescence, two-photon absorption, and two-photon excited fluorescence, were systematically investigated in various solvents. The results demonstrate that all the compounds emit relatively strong blue/cyan fluorescence. **1BN** and **5MOBI** exhibit large two-photon absorption cross-sections (471 and 654 GM) in THF. In addition, the relationship between the electronic structures and photophysical properties was investigated using density functional theory.

**Keywords:** Photophysical property; Blue/cyan fluorescence; Phenanthroline derivative; Green synthesis

---

\*Corresponding author. Tel. : +86 571 88320891.

E-mail address: [caizbmail@126.com](mailto:caizbmail@126.com) (Z.-B. Cai).

## 1. Introduction

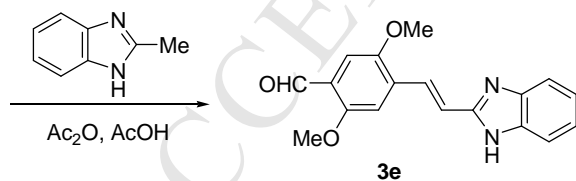
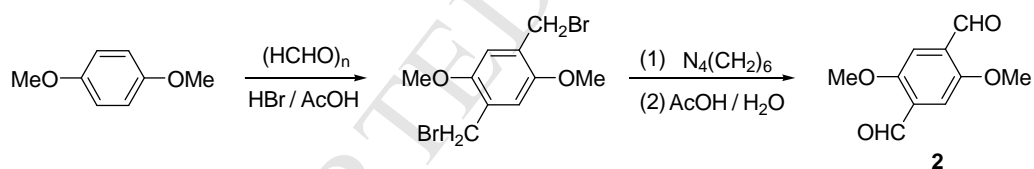
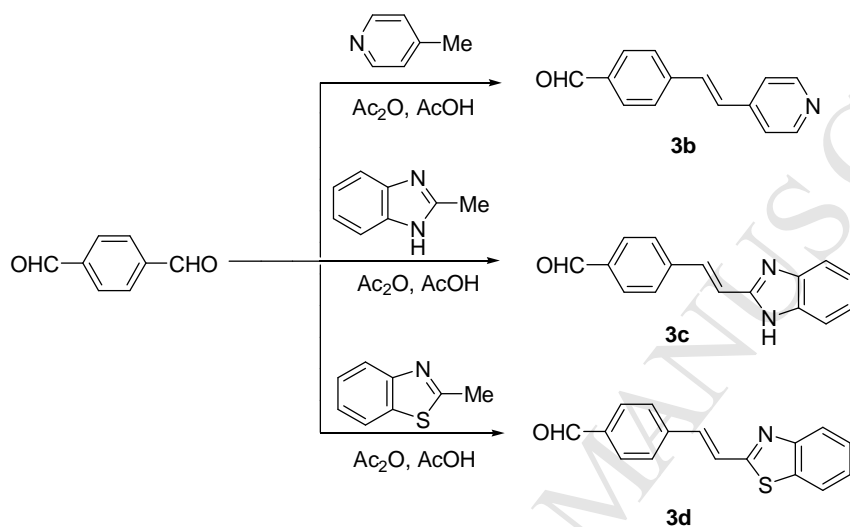
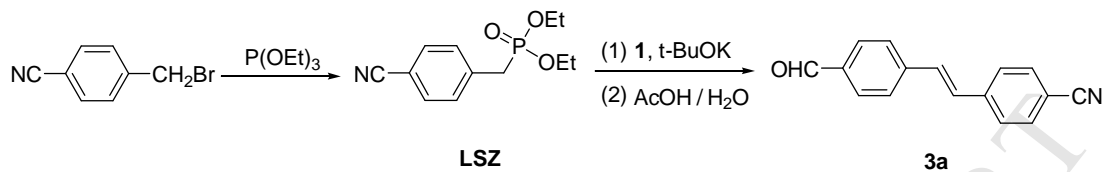
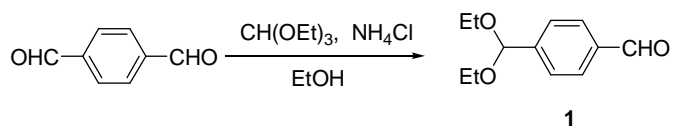
Two-photon absorption (TPA) is a third-order nonlinear optical process wherein two photons are absorbed simultaneously. The development of organic materials with large TPA cross-sections ( $\sigma$ ) has attracted considerable interest in the past decades due to a variety of potential applications in fields such as two-photon pumped up-converted lasing,<sup>1,2</sup> fluorescence imaging,<sup>3,4</sup> three-dimensional (3D) microfabrication,<sup>5,6</sup> 3D optical data storage,<sup>7-9</sup> optical limiting,<sup>10-12</sup> and photodynamic therapy.<sup>13-15</sup> Increasing the conjugated system is one of the commonly used strategies in the molecular design of TPA materials.<sup>16,17</sup> However, enhancement of the conjugated system will lead to a conflict between nonlinearity and transparency. That is, an increase in the conjugated system will cause a significant red-shift of the absorption wavelength, which will lead to a red-shift of the emission wavelength, usually to the green, yellow, or red light region. The blue-emitting TPA materials have some important applications. For example, they promote the development of the multi-channel two-photon induced fluorescence microscopy, which is helpful in reducing background light scattering and auto-fluorescence when probing natural molecules.<sup>18,19</sup> Up till now, the number of reported TPA materials with efficient blue emission is relatively limited. He et al.<sup>20</sup> designed four 1,8-diazapyrenes, for which the wavelengths of two-photon excited fluorescence (TPEF) are in the deep-blue light region, and the maximum two-photon cross-section ( $\sigma$ ) is 298 GM (1 GM =  $1 \times 10^{-50} \text{ cm}^4 \text{ s photon}^{-1}$ ). Cao et al.<sup>21</sup> synthesized a new A- $\pi$ -D- $\pi$ -A compound (A = acceptor, D = donor, and  $\pi$  = conjugated bridge), which exhibits blue-violet TPEF with a maximum  $\sigma$  value of 38 GM. Hu et al.<sup>22</sup> synthesized two novel  $\pi$ -conjugated carbazole derivatives with blue TPEF, with a maximum  $\sigma$  value of 49 GM. In order to

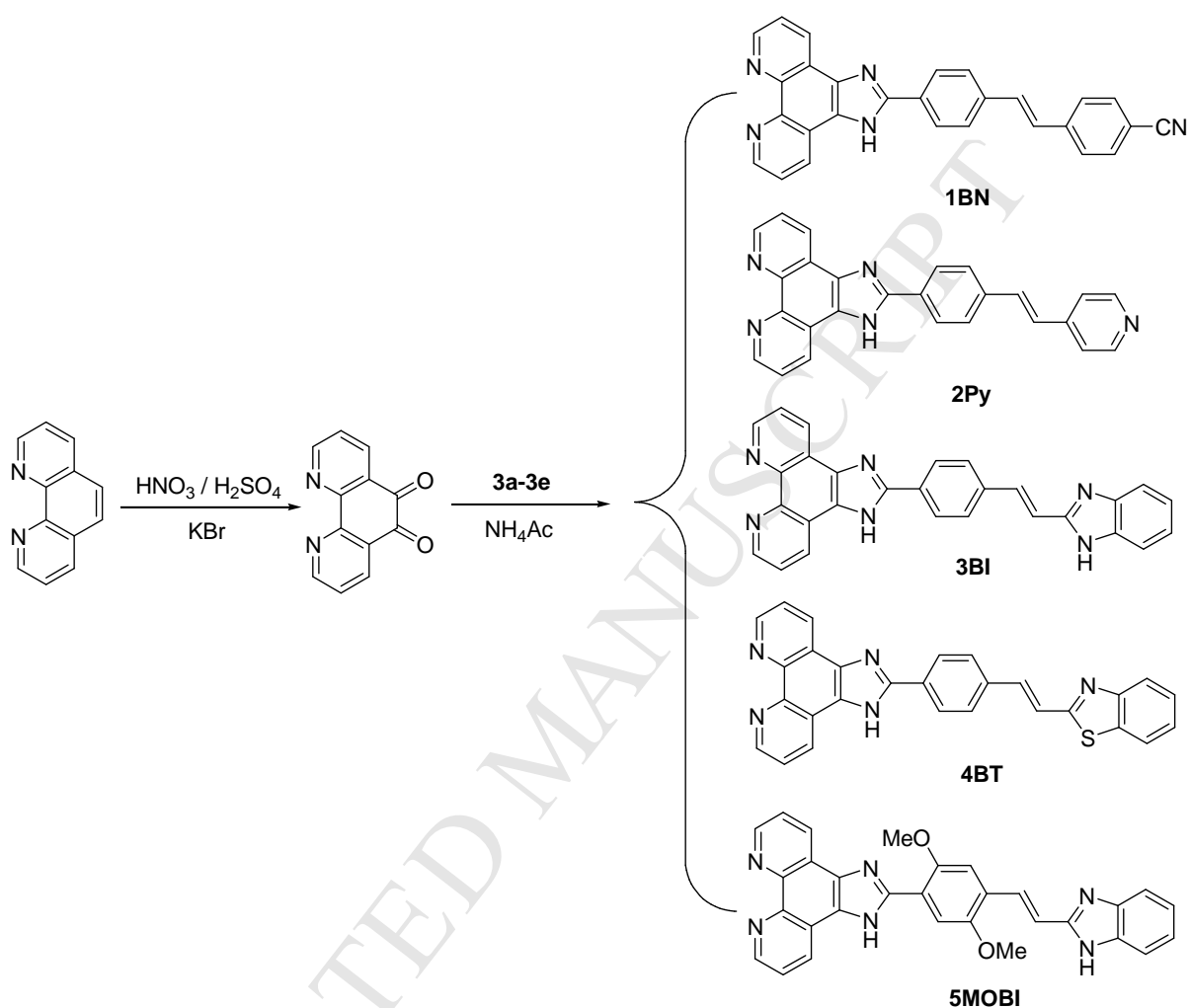
realize practical applications, the  $\sigma$  values of this kind of materials must be further improved. We think that appropriate conjugated structural units can play important roles in obtaining high-performance TPA materials that emit blue fluorescence.

1*H*-Imidazo[4,5-*f*][1,10]phenanthroline has a large planar structure, high electron-withdrawing ability, good electron transportability, high thermal stability, and good fluorescence properties. Its derivatives are widely used as luminescent materials,<sup>23</sup> biomolecular probes,<sup>24</sup> and molecular recognition.<sup>25</sup> In this study, we selected 1*H*-imidazo[4,5-*f*][1,10]phenanthroline as the effective conjugated structural unit, combining *trans* double bonds and various electron acceptors (benzonitrile, pyridine, benzimidazole, and benzothiazole) to synthesize four A- $\pi$ -A' compounds (**1BN**, **2Py**, **3BI**, and **4BT**) and one A-D- $\pi$ -A' compound (**5MOBI**). The introduction of a *trans*-diarylethene at the 2-position of the imidazole leads to an appropriate extension of the conjugated system, which may not only help to increase the fluorescence quantum yield ( $\Phi$ ) and  $\sigma$ , but also ensure that TPEF occurs in the blue light region. Till now, the compounds reported with similar structures are fairly rare,<sup>26-29</sup> and none of them exhibit blue fluorescence.

This kind of materials is usually synthesized by a Debus-Radziszewski reaction with diketones, aldehydes, and ammonium acetate as raw materials, and AcOH as the solvent. As this method usually produces a large amount of waste acid, it is not only difficult to conduct, but is very environmentally unfriendly. In this study, the target compounds were synthesized under solvent-free and catalyst-free conditions with relatively high selectivity and yields, which protects the environment, reduces the production cost, and simplifies the operation steps. Therefore, it can be considered as an efficient synthesis method.

The linear and nonlinear photophysical properties of the target compounds have been systematically investigated in different solvents. Furthermore, density functional theory (DFT) calculations have been employed to study the structure-property relationships of the target compounds, which provides a reference for the development of high-performance TPA materials that emit blue fluorescence.





**Scheme 1.** Synthetic route of the target compounds (**1BN**, **2Py**, **3BI**, **4BT**, and **5MOBI**).

## 2. Results and discussion

### 2.1. Synthesis and characterization

The synthetic routes of the target compounds (**1BN**, **2Py**, **3BI**, **4BT**, and **5MOBI**) are depicted in Scheme 1. 4-[(1*E*)-2-(4-Formylphenyl)ethenyl]benzonitrile (**3a**) was prepared by a two-step reaction, which involved the Horner–Wadsworth–Emmons reaction between 4-(diethoxymethyl)benzaldehyde (**1**) and

[(4-cyanophenyl)methyl]phosphonic acid diethyl ester (**LSZ**) using potassium *tert*-butoxide as the catalyst, followed by hydrolysis in acetic acid. The other four intermediates, 4-[(1*E*)-2-(4-pyridinyl)ethenyl]benzaldehyde (**3b**), 4-[(1*E*)-2-(1*H*-benzimidazol-2-yl)ethenyl]benzaldehyde (**3c**), 4-[(1*E*)-2-(2-benzothiazolyl)ethenyl]benzaldehyde (**3d**), and 4-[(1*E*)-2-(1*H*-benzimidazol-2-yl)ethenyl]-2,5-dimethoxybenzaldehyde(**3e**), were synthesized by acid condensation of 4-methylpyridine, 2-methyl-1*H*-benzimidazole, or 2-methylbenzothiazole with 1,4-benzenedicarboxaldehyde or 2,5-dimethoxy-1,4-benzenedicarboxaldehyde (**2**). Finally, the solvent-free Debus–Radziszewski reaction of **3a–3e** with 1,10-phenanthroline-5,6-dione gave the target compounds (**1BN**, **2Py**, **3BI**, **4BT**, and **5MOBI**) in relatively high yields (67.5%–78.9%). This solvent-free reaction offers considerable advantages such as simplified operation, lower production cost, and environmental friendliness, and thus significantly contributes to the practice of green chemistry.

In the <sup>1</sup>H NMR spectra, the chemical shifts ( $\delta$ ) of the target compounds (**1BN**, **2Py**, **3BI**, **4BT**, and **5MOBI**) at 13.02–13.89 ppm were detected as broad singlets, which were attributed to the N-H in the imidazole moiety. In addition, the observed *J* coupling constants for the vinyl protons of the compounds were in the range of 16.3–16.5 Hz, which is consistent with the expected values for an all-*trans* configuration. The N-H in the imidazole moiety was also identified by FT-IR spectroscopy as bands within the spectral region of 3332–3398 cm<sup>-1</sup>. Mass spectrometry was used to further verify the structures of the compounds. For the five molecules, the observed values agreed well with the calculated values.

## 2.2 Linear absorption and emission properties

The photophysical properties for all the target compounds (**1BN**, **2Py**, **3BI**, **4BT**, and **5MOBI**) are summarized in Table 1. Their linear absorption spectra in tetrahydrofuran (THF) are shown in Fig. 1.

Table 1 Linear and nonlinear photophysical properties of the target compounds (**1BN**, **2Py**, **3BI**, **4BT**, and **5MOBI**).

Compound	Solvent	$\lambda_{\max}^{\text{abs}}$ <sup>a</sup> (nm)	$10^{-4}\epsilon$ <sup>b</sup> (mol <sup>-1</sup> L cm <sup>-1</sup> )	$\lambda_{\max}^{\text{OPEF}}$ <sup>c</sup> (nm)	$\Delta\nu$ <sup>d</sup> (cm <sup>-1</sup> )	$\phi$ <sup>e</sup>	$\lambda_{\max}^{\text{TPEF}}$ <sup>f</sup> (nm)	$\sigma$ <sup>g</sup> (GM)
<b>1BN</b>	THF	376	10.97	463	4997	0.42	506	471
	CH <sub>2</sub> Cl <sub>2</sub>	377	6.09	467	5112	0.34		
	CH <sub>3</sub> CN	368	10.26	471	5942	0.26		
	CH <sub>3</sub> OH	360	10.66	473	6636	0.16	508	251
<b>2Py</b>	THF	367	11.28	449	4976	0.54	503	270
	CH <sub>2</sub> Cl <sub>2</sub>	363	4.89	456	5618	0.48		
	CH <sub>3</sub> CN	357	7.93	461	6319	0.32		
	CH <sub>3</sub> OH	349	6.48	469	7331	0.19	508	194
<b>3BI</b>	THF	381	13.45	444	3724	0.11	488	209
	CH <sub>2</sub> Cl <sub>2</sub>	382	9.86	447	3807	0.07		
	CH <sub>3</sub> CN	376	8.67	450	4374	0.15		
	CH <sub>3</sub> OH	375	9.53	452	4573	0.09	492	94
<b>4BT</b>	THF	386	13.44	469	4585	0.33	515	349
	CH <sub>2</sub> Cl <sub>2</sub>	384	9.98	472	4855	0.25		
	CH <sub>3</sub> CN	380	8.00	485	5697	0.17		
	CH <sub>3</sub> OH	375	6.05	488	6175	0.11	521	197
<b>5MOBI</b>	THF	401	14.10	443	2364	0.75	496	654
	CH <sub>2</sub> Cl <sub>2</sub>	400	12.19	452	2876	0.62		

CH <sub>3</sub> CN	398	6.46	457	3244	0.43		
CH <sub>3</sub> OH	391	3.23	461	3883	0.21	499	370

- <sup>a</sup> Maximum linear absorption wavelength,  $c = 1 \times 10^{-5} \text{ mol L}^{-1}$ .
- <sup>b</sup> Maximum molar absorption coefficient.
- <sup>c</sup> Maximum one-photon excited fluorescence wavelength,  $c = 1 \times 10^{-6} \text{ mol L}^{-1}$ .
- <sup>d</sup> Stokes shift.
- <sup>e</sup> Fluorescence quantum yield, measured by using quinine sulfate in  $0.5 \text{ mol L}^{-1}$  sulfuric acid as the standard ( $\Phi = 0.546$ <sup>30</sup>).
- <sup>f</sup> Maximum two-photon excited fluorescence wavelength,  $c = 1 \times 10^{-3} \text{ mol L}^{-1}$ .
- <sup>g</sup> Two-photon absorption cross-section.

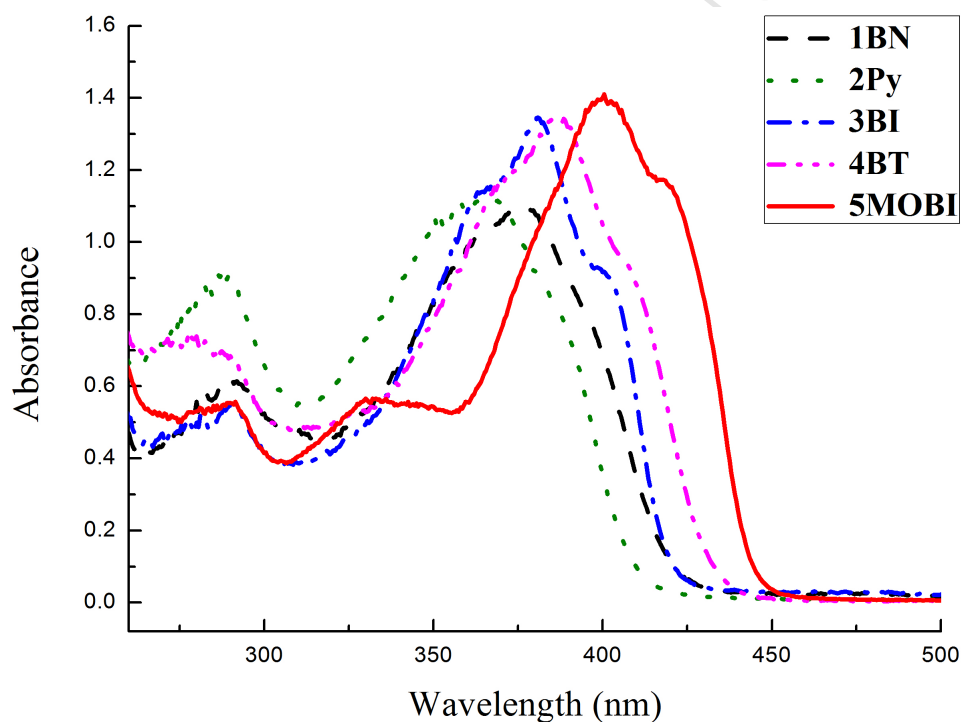


Fig. 1 Linear absorption spectra of the target compounds (**1BN**, **2Py**, **3BI**, **4BT**, and **5MOBI**) in THF with a concentration of  $1 \times 10^{-5} \text{ mol L}^{-1}$ .

As shown in Fig. 1, **1BN**, **2Py**, **3BI**, and **4BT** exhibit two absorption bands, while **5MOBI** shows three obvious bands. The high-energy absorption bands (278–291 nm) for all the compounds can be ascribed to the  $\pi$ - $\pi^*$  transition of the

1*H*-imidazo[4,5-*f*][1,10]phenanthroline. The low-energy bands around 367–401 nm result from the internal charge transfer (ICT) process. Whereas the absorption band at 330 nm of **5MOBI** can be attributed to the  $n-\pi^*$  transition of the oxygen atoms. The absorption spectra of all the target compounds (**1BN**, **2Py**, **3BI**, **4BT**, and **5MOBI**) exhibit obvious blue-shifts in methanol, but show only limited solvent polarity dependencies in the other three solvents. This blue-shift could be explained by the hydrogen bonds between the solute and methanol molecules, which results in the energy gap increasing between the ground state  $S_0$  and the excited state  $S_1$ . The absorption peak positions ( $\lambda_{\max}^{\text{abs}}$ ) of these compounds follow the order **5MOBI** > **4BT** > **3BI** > **1BN** > **2Py**. There is a prominent red-shift from **3BI** to its methoxy substituted compound (**5MOBI**), implying that the introduction of electron donor is beneficial to reduce the absorption energy. The maximum molar absorption coefficients ( $\epsilon_{\max}$ ) of the target compounds in THF are higher than those of the other three solvents, which indicates that they have the strongest light absorbing ability in THF.

The one-photon excited fluorescence (OPEF) spectra and fluorescence photographs of the target compounds (**1BN**, **2Py**, **3BI**, **4BT**, and **5MOBI**) in THF are shown in Fig. 2 and the corresponding data are summarized in Table. 1. All the target compounds emit blue/cyan fluorescence. Upon increasing the polarity of the solvent, their fluorescent emission peaks ( $\lambda_{\max}^{\text{OPEF}}$ ) show remarkable bathochromic shifts. This red-shifted behavior is accompanied by an increase in the Stokes shifts ( $\Delta\nu$ ) when the polarity of the solvent increases. This can be attributed to the fact that the excited state may possess a higher polarity than the ground state. An increased dipole-dipole interaction between the solute and solvent leads to a lowering of the energy level of the excited state.<sup>31,32</sup> The OPEF spectra of **3BI** and **5MOBI** exhibit two emission peaks in the medium polar solvent (THF). The emission peaks at 422 nm (**3BI**) and 443 nm (**5MOBI**) are assigned to the locally excited (LE) state, and the longer emission wavelengths centered at 444 nm (**3BI**) and 469 nm (**5MOBI**) are assigned to the ICT state.

The  $\Phi$  values in different solvents were determined using quinine sulfate as standard. As seen in Table. 1, the  $\Phi$  values in the four solvents change slightly for **3BI**. However, the  $\Phi$  values of **1BN**, **2Py**, **4BT**, and **5MOBI** decrease significantly upon increasing the solvent polarity. The origin of this phenomenon can be attributed to “twisted intramolecular charge transfer (TICT)”<sup>33</sup> in the excited state. The TICT state is much less emissive and strongly dependent on the polarity of solvents. An increase in the solvent polarity can lead to an enhanced TICT process and causes greater energy loss from the excited state.<sup>34,35</sup>

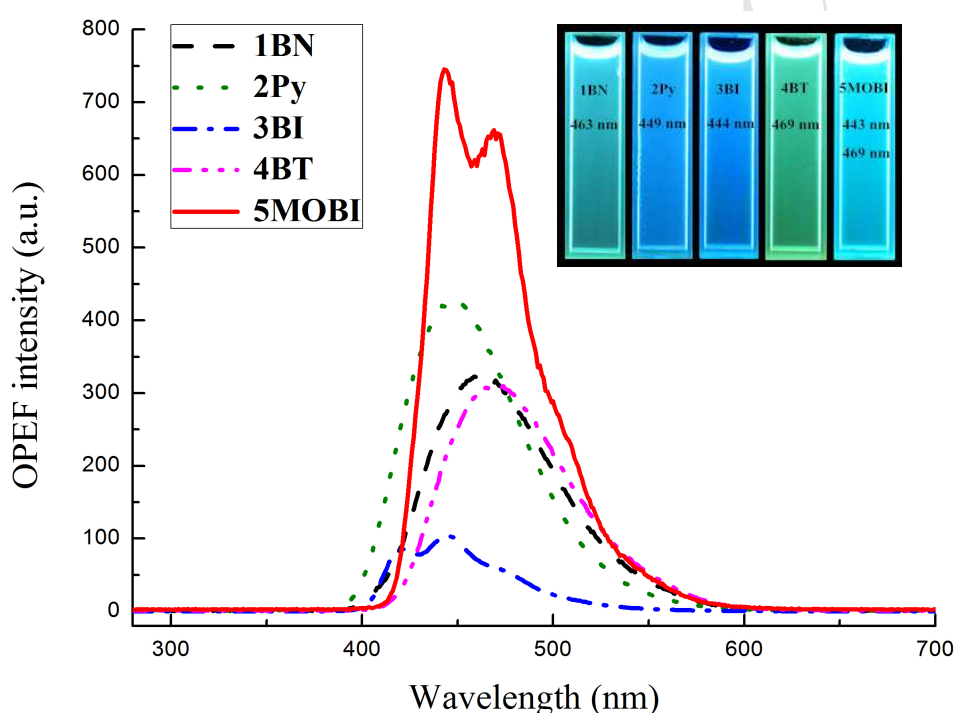


Fig. 2 OPEF spectra and fluorescence photographs of the target compounds (**1BN**, **2Py**, **3BI**, **4BT**, and **5MOBI**) in THF with a concentration of  $1 \times 10^{-6}$  mol L<sup>-1</sup>.

### 2.3 Two-photon properties

The nonlinear photophysical data of the target compounds (**1BN**, **2Py**, **3BI**, **4BT**, and **5MOBI**) are listed in Table. 1, which were measured in THF and methanol ( $c = 1 \times 10^{-3}$  mol L<sup>-1</sup>). The representative TPEF spectra of **5MOBI** in THF, pumped by femtosecond laser pulses at 500 mW under different excitation wavelengths, are presented in Fig. 3. By comparing the peak positions of TPEF ( $\lambda_{\max}^{\text{TPEF}}$ ) with those of

OPEF ( $\lambda_{\max}^{\text{OPEF}}$ ) for the target compounds, one can observe that  $\lambda_{\max}^{\text{TPEF}}$  values are red-shifted by 28–54 nm. These red-shifts are attributed to the reabsorption effect of the fluorescence within the solutions.<sup>36</sup>

As shown in Fig. 1, there is no linear absorption in the wavelength range of 500–1000 nm for the five compounds, which indicates that there are no molecular energy levels corresponding to an electron transition in this spectral range. Therefore, on excitation from 690 to 850 nm, it is impossible to produce one-photon excited fluorescence. If up-converted fluorescence induced with a laser appears, it could be ascribed to TPEF. Fig.4 shows the TPEF spectra of **5MOBI** under different pump powers and the logarithmic plot of the output fluorescence integral versus the input powers. The logarithmic plot has a slope of 2.0673 as the input laser power is increased, suggesting a two-photon excitation mechanism. The other compounds (**1BN**, **2Py**, **3BI**, and **4BT**) are also proved to have the same excitation mechanism.

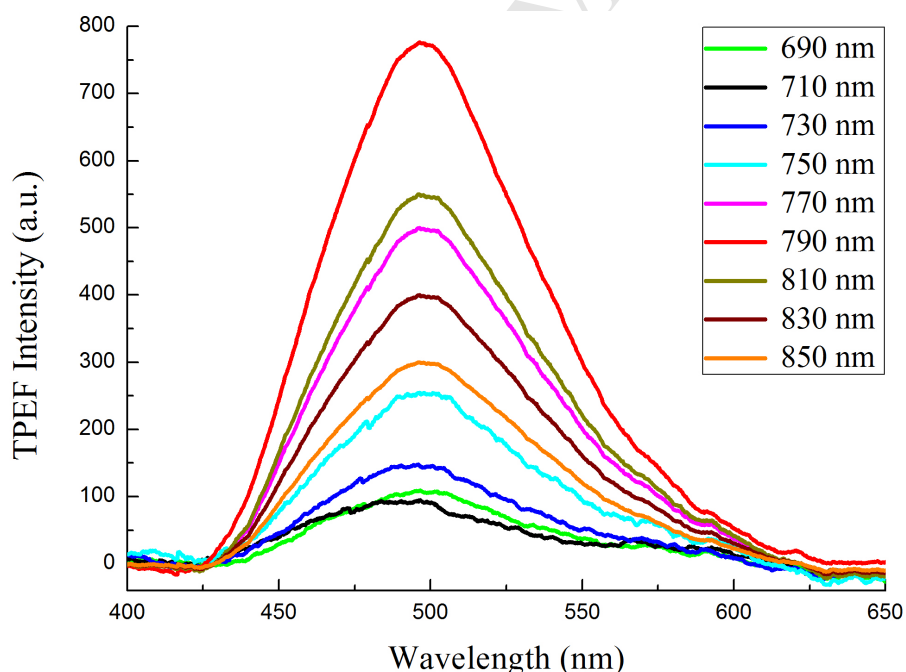


Fig. 3 TPEF spectra of **5MOBI** in THF pumped by femtosecond laser pulses at 500 mW under different excitation wavelengths.

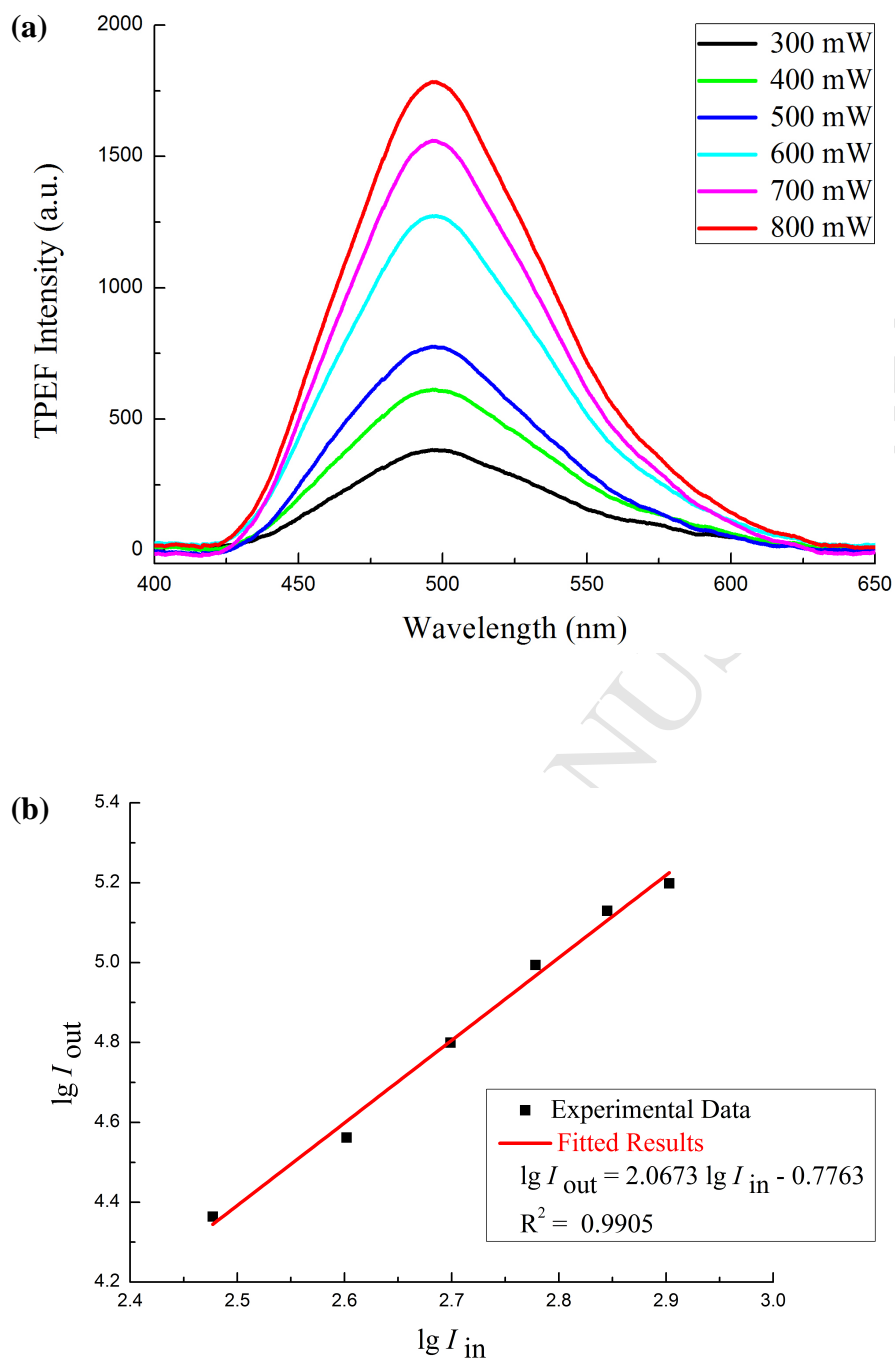


Fig. 4 (a) TPEF spectra of **5MOBI** in THF at 790 nm under different input powers. (b) Logarithmic plot of the output fluorescence integral ( $I_{out}$ ) versus the input laser powers ( $I_{in}$ ).

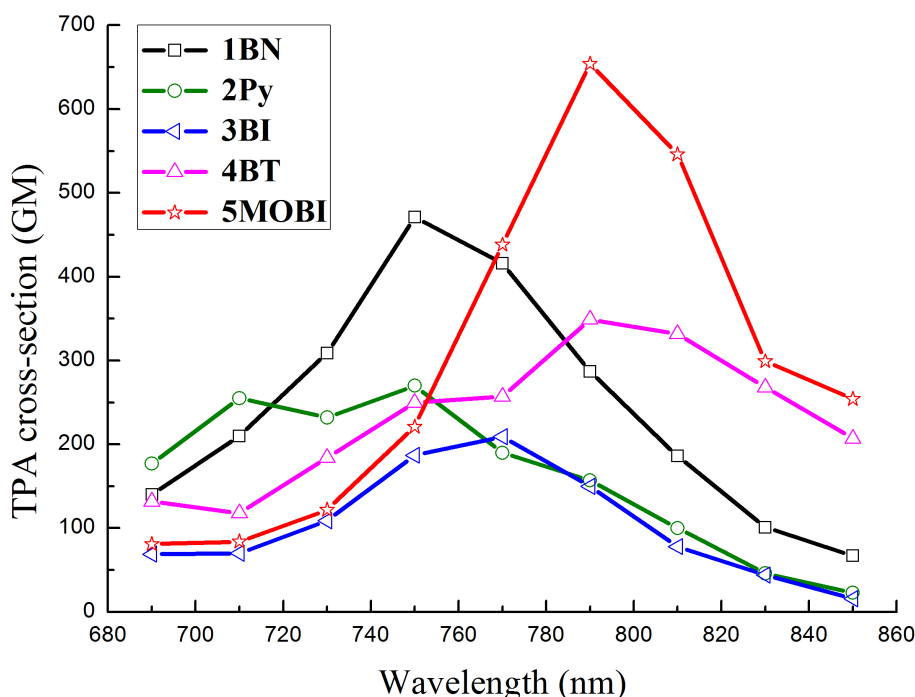


Fig. 5 TPA cross-sections of the target compounds (**1BN**, **2Py**, **3BI**, **4BT**, and **5MOBI**) in THF.

The  $\sigma$  values of the five target compounds were determined in the wavelength range from 690 to 850 nm, using a two-photon induced fluorescence measurement technique. As shown in Table 1 and Fig. 5, the maximum  $\sigma$  values in THF are 471 GM for **1BN**, 270 GM for **2Py**, 209 GM for **3BI**, 349 GM for **4BT**, and 654 GM for **5MOBI**, respectively, which are larger than those in methanol (251 GM for **1BN**, 194 GM for **2Py**, 94 GM for **3BI**, 197 GM for **4BT**, and 370 GM for **5MOBI**). The  $\sigma$  value of **5MOBI** is more than three times as large as that of **3BI**, this can be attributed to the following reasons: **3BI** is an A- $\pi$ -A' compound where electron-withdrawing imidazophenanthroline and benzimidazole are bound at opposite ends of styrene conjugated bridge. As for **5MOBI**, two electron-donating methoxy groups are introduced at the 2- and 5-positions of the benzene ring to form an A-D- $\pi$ -A' configuration. The introduction of the electron donors produces the multidirectional charge transfer, which results in higher degree of electron delocalization, and finally enlarges the  $\sigma$  value obviously.

A three-level model is generally utilized to describe the TPA properties of the

molecules, in which TPA into high-lying states is not dipole coupled to the ground state. It can be written as Equation (1):<sup>20</sup>

$$\sigma = \frac{M_{01}^2 M_{12}^2}{(E_1 - E_0 - \hbar\omega)^2 \Gamma} \quad (1)$$

Where  $M_{01}$  and  $M_{12}$  are the transition dipole moments from  $S_0$  to  $S_1$  and  $S_1$  to  $S_2$ , respectively.  $\hbar\omega = (E_2 - E_0)/2$ ,  $E_0$ ,  $E_1$ , and  $E_2$  represent the corresponding energy of  $S_0$ ,  $S_1$ , and  $S_2$ .  $\Gamma$  is the damping factor.

Some studies have demonstrated that  $\sigma$  is related to the extent of ICT through the  $\pi$ -bridge in the molecule,<sup>37</sup> and according to the equation (1),  $\sigma$  shows negative correlation with the transition energy  $\Delta E_{01}$  ( $\Delta E_{01} = E_1 - E_0$ ). Therefore, theoretical studies based on DFT calculations using the Gaussian 09 program<sup>38</sup> at the B3LYP/6-31G level<sup>39</sup> of theory were conducted for optimization of the target compounds in order to gain an insight into the relationship between the  $\sigma$  of the compounds and the distribution of the electron densities over the molecules. The frontier molecular orbitals for the five compounds are depicted in Fig. 6. The corresponding  $\Delta E$  values of the target compounds were calculated to be 3.11 (**1BN**), 3.28 (**2Py**), 3.20 (**3BI**), 3.15 (**4BT**), and 3.11 (**5MOBI**) eV, respectively. For all the target compounds, the electron densities in the highest occupied molecular orbital (HOMO) are delocalized over the entire molecule, whereas the distributions of the lowest unoccupied molecular orbital (LUMO) appear to be different. For **5MOBI**, in the LUMO, the electron clouds on imidazophenanthroline, benzimidazole, and methoxy groups are partly transferred to the styrene  $\pi$ -bridge. This multidirectional charge transfer and a relatively small  $\Delta E$  (3.11 eV) obviously improve the TPA ability, resulting in the largest  $\sigma$ .

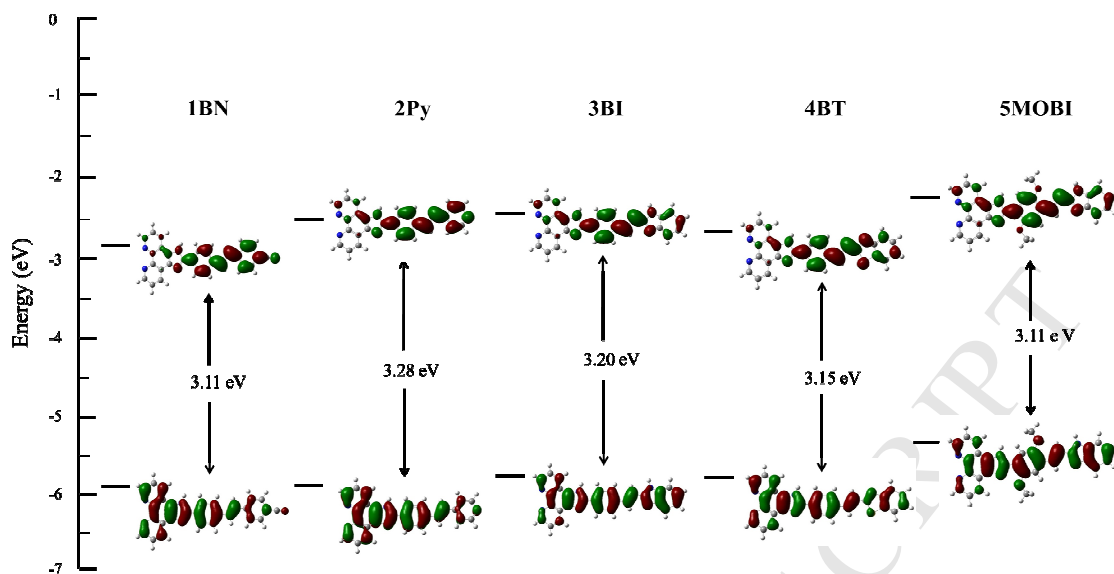


Fig. 6 Molecular orbital energy level diagram for the target compounds (**1BN**, **2Py**, **3BI**, **4BT**, and **5MOBI**).

### 3. Conclusion

In this study, five new 1*H*-imidazo[4,5-*f*]phenanthroline derivatives were synthesized by a solvent-free Debus–Radziszewski reaction. Their linear and nonlinear photophysical properties were systematically investigated in various solvents. All the compounds exhibit relatively large  $\sigma$  values and strong blue/cyan fluorescence.

## 4. Experimental section

### 4.1. General procedures

All the reagents and solvents were commercially purchased and used without further purification.  $^1\text{H}$  and  $^{13}\text{C}$  NMR spectra were recorded on a Bruker AVANCE III 500 spectrometer using  $\text{DMSO-}d_6$  as a solvent and all shifts are referred to tetramethylsilane (TMS). FT-IR spectra were recorded on a Thermo Nicolet 6700 spectrometer using a powder sample on a KBr plate. Mass spectra were performed on a Therm LCQ TM Deca XP plus ion trap mass spectrometry instrument. Elemental

analyses were determined by a Thermo Finnigan Flash EA 1112 apparatus.

## 4.2. Spectroscopic measurements

The OPA spectra were recorded on a Shimadzu UV-2550 UV-visible spectrophotometer. The OPEF spectra were performed using a RF-5301PC fluorescence spectrophotometer. The  $\Phi$  were determined by using quinine sulfate in 0.5 mol L<sup>-1</sup> sulfuric acid as the standard ( $\Phi = 0.546^{30}$ ).  $\Phi$  is calculated according to the following equation:

$$\Phi_s = \Phi_r \frac{A_r n_s^2 F_s}{A_s n_r^2 F_r} \quad (2)$$

where the subscripts s and r designate the sample and the reference, respectively.  $A$  is the absorbance at the excitation wavelength,  $n$  is the refractive index of the relevant solution, and  $F$  is the integrated area under the corrected emission spectrum.

The TPEF spectra were measured using a femtosecond laser pulse and a Ti:sapphire system (680–1080 nm, 80 MHz, 140 fs) as the light source.  $\sigma$  of the target compounds were measured using the two-photon induced fluorescence method with the following equation :

$$\sigma_s = \frac{F_s \phi_r n_r c_r}{F_r \phi_s n_s c_s} \sigma_r \quad (3)$$

where the subscripts s and r denote the sample and the reference, respectively.  $F$  and  $\Phi$  represent the TPEF integral intensity and the fluorescence quantum yield.  $n$  and  $c$  are the refractive index and the concentration of the solution. In this work, fluorescein in 0.1 mol L<sup>-1</sup> sodium hydroxide ( $c = 1 \times 10^{-3}$  mol L<sup>-1</sup>) is used as the reference ( $\sigma = 36$  GM<sup>40</sup>).

## 4.3 Synthesis

The synthetic routes of the expected compounds are depicted in Scheme 1. 2,5-Dimethoxy-1,4-benzenedicarboxaldehyde (**2**),<sup>41</sup> 1,10-phenanthroline-5,6-dione,<sup>42</sup> [(4-cyanophenyl)methyl]phosphonic acid diethyl ester (**LSZ**),<sup>43</sup> 4-[(1E)-2-(4-formylphenyl)ethenyl]benzonitrile (**3a**),<sup>44</sup> 4-[(1E)-2-(4-pyridinyl)ethenyl]benzaldehyde (**3b**),<sup>45</sup> 4-[(1E)-2-(1H-benzimidazol-2-yl)ethenyl]benzaldehyde (**3c**),<sup>46</sup> 4-[(1E)-2-(2-benzothiazolyl)ethenyl]benzaldehyde (**3d**),<sup>46</sup> and

4-[(1*E*)-2-(1*H*-benzimidazol-2-yl)ethenyl]-2,5-dimethoxybenzaldehyde (**3e**)<sup>47</sup> were synthesized according to the literature procedures.

4.3.1 4-[(1*E*)-2-[4-(1*H*-imidazo[4,5-*f*][1,10]phenanthrolin-2-yl)phenyl]ethenyl] benzonitrile (**1BN**)

A mixture of 1,10-phenanthroline-5,6-dione (1 mmol, 0.21 g), **2a** (1 mmol, 0.23g), and ammonium acetate (5 mmol, 0.39 g) was ground into powder in a mortar and then heated at 80 °C for 8 h. After completion of the reaction (monitored by TLC), the reaction mixture was cooled to room temperature and treated with water. The resulting solid was purified by recrystallization from N,N-dimethylformamide to give 0.32 g orange–yellow crystalline powder. Yield 75.2 %. m.p. > 300 °C; <sup>1</sup>H NMR (DMSO-*d*<sub>6</sub>, 500 MHz) δ: 13.83 (s, 1H), 9.07 (dd, *J*<sub>1</sub> = 4.0 Hz, *J*<sub>2</sub> = 1.2 Hz, 2H), 8.97 (dd, *J*<sub>1</sub> = 8.1 Hz, *J*<sub>2</sub> = 1.2 Hz, 2H), 8.35 (d, *J* = 8.3 Hz, 2H), 7.92 (d, *J* = 8.3 Hz, 2H), 7.89 (d, *J* = 8.5 Hz, 2H), 7.87 (br s, 2H), 7.86 (d, *J* = 8.5 Hz, 2H), 7.60 (d, *J* = 16.4 Hz, 1H), 7.52 (d, *J* = 16.4 Hz, 1H); <sup>13</sup>C NMR (DMSO-*d*<sub>6</sub>, 125 MHz) δ: 109.69, 119.02, 123.32, 126.55, 127.27, 127.61, 127.84, 129.65, 129.67, 129.70, 131.49, 132.69, 135.69, 137.54, 141.73, 143.69, 147.92, 150.07; FT-IR (KBr) ν: 3334, 3030, 2854, 2222, 1653, 1599, 1559, 1506, 1480, 1451, 1397, 1351, 1175, 1070, 949, 837, 739, 554 cm<sup>-1</sup>; ESI-MS *m/z*: 424.28 [M+H]<sup>+</sup>, 446.25 [M+Na]<sup>+</sup>; Anal. calcd for C<sub>28</sub>H<sub>17</sub>N<sub>5</sub>: C 79.42, H 4.05, N 16.54; found C 79.61, H 4.12, N 16.78.

4.3.2 4-[(1*E*)-2-[4-(1*H*-imidazo[4,5-*f*][1,10]phenanthrolin-2-yl)phenyl]ethenyl] pyridine (**2Py**). **2Py** was synthesized as that of **1BN**. Orange-yellow crystalline powder. Yield 71.1 %. m.p. 240–242 °C; <sup>1</sup>H NMR (DMSO-*d*<sub>6</sub>, 500 MHz) δ: 13.84 (s, 1H), 9.07 (dd, *J*<sub>1</sub> = 4.3 Hz, *J*<sub>2</sub> = 1.5 Hz, 1H), 9.06 (dd, *J*<sub>1</sub> = 4.3 Hz, *J*<sub>2</sub> = 1.5 Hz, 1H), 8.97 (dd, *J*<sub>1</sub> = 8.0 Hz, *J*<sub>2</sub> = 1.5 Hz, 1H), 8.96 (dd, *J*<sub>1</sub> = 8.0 Hz, *J*<sub>2</sub> = 1.5 Hz, 1H), 8.60 (d, *J* = 6.0 Hz, 2H), 8.36 (d, *J* = 8.4 Hz, 2H), 7.93 (d, *J* = 8.4 Hz, 2H), 7.90 (dd, *J*<sub>1</sub> = 8.0 Hz, *J*<sub>2</sub> = 4.3 Hz, 1H), 7.85 (dd, *J*<sub>1</sub> = 8.0 Hz, *J*<sub>2</sub> = 4.3 Hz, 1H), 7.67 (d, *J* = 16.4 Hz, 1H), 7.63 (d, *J* = 6.0 Hz, 2H), 7.43 (d, *J* = 16.4 Hz, 1H); <sup>13</sup>C NMR (DMSO-*d*<sub>6</sub>, 125 MHz) δ: 120.99, 121.17, 123.49, 126.60, 127.04, 127.75, 129.72, 129.77, 129.86, 132.32, 135.85, 135.89, 137.34, 143.60, 143.67, 144.17, 147.94, 150.13, 150.17;

FT-IR (KBr)  $\nu$ : 3332, 3076, 2850, 1624, 1600, 1560, 1501, 1484, 1424, 1399, 1195, 1072, 955, 839, 740  $\text{cm}^{-1}$ ; ESI-MS  $m/z$ : 400.29  $[\text{M}+\text{H}]^+$ , 422.36  $[\text{M}+\text{Na}]^+$ ; Anal. calcd for  $\text{C}_{26}\text{H}_{17}\text{N}_5$ : C 78.18, H 4.29, N 17.53; found C 78.41, H 4.39, N 17.82.

4.3.3 2-[(1E)-2-[4-(1H-imidazo[4,5-f][1,10]phenanthrolin-2-yl)phenyl]ethenyl]-1H-benzimidazole (**3BI**). **3BI** was synthesized as that of **1BN**. Orange-yellow crystalline powder. Yield 71.8 %. m.p. > 300 °C;  $^1\text{H}$  NMR (DMSO- $d_6$ , 500 MHz)  $\delta$ : 13.85 (br s, 1H), 12.72 (s, 1H), 9.06 (dd,  $J_1 = 4.3$  Hz,  $J_2 = 1.6$  Hz, 2H), 8.96 (dd,  $J_1 = 8.1$  Hz,  $J_2 = 1.6$  Hz, 2H), 8.37 (d,  $J = 8.4$  Hz, 2H), 7.94 (d,  $J = 8.4$  Hz, 2H), 7.87 (br s, 2H), 7.76 (d,  $J = 16.5$  Hz, 1H), 7.64 (d,  $J = 7.7$  Hz, 1H), 7.53 (d,  $J = 7.7$  Hz, 1H), 7.39 (d,  $J = 16.5$  Hz, 1H), 7.16-7.23 (m, 2H);  $^{13}\text{C}$  NMR (DMSO- $d_6$ , 125 MHz)  $\delta$ : 118.72, 119.30, 123.19, 123.49, 123.72, 126.60, 126.68, 127.68, 129.66, 129.71, 129.95, 133.45, 135.94, 135.96, 136.92, 141.90, 143.62, 143.76, 147.94, 147.99, 150.08; FT-IR (KBr)  $\nu$ : 3365, 3084, 2933, 1641, 1609, 1564, 1526, 1481, 1425, 1393, 1278, 1071, 969, 827, 740  $\text{cm}^{-1}$ ; ESI-MS  $m/z$ : 439.23  $[\text{M}+\text{H}]^+$ , 461.29  $[\text{M}+\text{Na}]^+$ ; Anal. calcd for  $\text{C}_{28}\text{H}_{18}\text{N}_6$ : C 76.70, H 4.14, N 19.17; found C 76.86, H 4.25, N 19.32.

4.3.4 2-[(1E)-2-[4-(1H-imidazo[4,5-f][1,10]phenanthrolin-2-yl)phenyl]ethenyl]benzothiazole (**4BT**). **4BT** was synthesized as that of **1BN**. Orange-yellow crystalline powder. Yield 78.9 %. m.p. > 300 °C;  $^1\text{H}$  NMR (DMSO- $d_6$ , 500 MHz)  $\delta$ : 13.89 (s, 1H), 9.07 (d,  $J = 4.0$  Hz, 2H), 8.98 (d,  $J = 8.0$  Hz, 2H), 8.37 (d,  $J = 8.3$  Hz, 2H), 8.14 (d,  $J = 7.9$  Hz, 1H), 8.07 (d,  $J = 8.3$  Hz, 2H), 8.02 (d,  $J = 8.1$  Hz, 1H), 7.91 (br s, 1H), 7.88 (br s, 1H), 7.81 (d,  $J = 16.3$  Hz, 1H), 7.77 (d,  $J = 16.3$  Hz, 1H), 7.55 (t,  $J = 7.6$  Hz, 1H), 7.47 (t,  $J = 7.6$  Hz, 1H);  $^{13}\text{C}$  NMR (DMSO- $d_6$ , 125 MHz)  $\delta$ : 122.20, 122.61, 122.69, 123.48, 123.51, 125.55, 125.58, 126.55, 128.35, 129.96, 130.45, 134.14, 136.28, 136.55, 143.17, 143.28, 147.73, 150.04, 151.88, 153.44, 166.32; FT-IR (KBr)  $\nu$ : 3335, 3051, 2862, 1623, 1603, 1559, 1484, 1435, 1396, 1315, 1109, 1070, 951, 819, 741  $\text{cm}^{-1}$ ; ESI-MS  $m/z$ : 456.21  $[\text{M}+\text{H}]^+$ , 478.34  $[\text{M}+\text{Na}]^+$ ; Anal. calcd for  $\text{C}_{28}\text{H}_{17}\text{N}_5\text{S}$ : C 73.83, H 3.76, N 15.37; found C 74.09, H 3.82, N 15.68.

4.3.5 2-[(1E)-2-[4-(1H-imidazo[4,5-f][1,10]phenanthrolin-2-yl)-2,5-dimethoxyphenyl]ethenyl]-1H-benzimidazole (**5MOBI**). **5MOBI** was synthesized as that of **1BN**. Yellow crystalline powder. Yield 67.5 %. m.p. > 300 °C; <sup>1</sup>H NMR (DMSO-*d*<sub>6</sub>, 500 MHz) δ: 13.02 (s, 1H), 12.75 (s, 1H), 9.23 (dd, *J*<sub>1</sub> = 8.1 Hz, *J*<sub>2</sub> = 1.5 Hz, 1H), 9.07 (dd, *J*<sub>1</sub> = 4.7 Hz, *J*<sub>2</sub> = 1.5 Hz, 1H), 9.05 (dd, *J*<sub>1</sub> = 4.6 Hz, *J*<sub>2</sub> = 1.5 Hz, 1H), 9.00 (dd, *J*<sub>1</sub> = 8.0 Hz, *J*<sub>2</sub> = 1.5 Hz, 1H), 8.00 (s, 1H), 7.99 (d, *J* = 16.5 Hz, 1H), 7.86 (dd, *J*<sub>1</sub> = 8.1 Hz, *J*<sub>2</sub> = 4.7 Hz, 1H), 7.84 (dd, *J*<sub>1</sub> = 8.0 Hz, *J*<sub>2</sub> = 4.6 Hz, 1H), 7.64 (s, 1H), 7.63 (d, *J* = 7.7 Hz, 1H), 7.51 (d, *J* = 16.5 Hz, 1H), 7.50 (d, *J* = 7.7 Hz, 1H), 7.17-7.24 (m, 2H), 4.15 (s, 3H), 4.05 (s, 3H); <sup>13</sup>C NMR (DMSO-*d*<sub>6</sub>, 125 MHz) δ: 56.29, 56.50, 110.43, 111.15, 112.47, 118.68, 119.40, 119.67, 122.96, 123.47, 123.62, 126.60, 128.26, 129.81, 130.44, 134.70, 134.86, 135.23, 140.29, 143.61, 143.82, 147.82, 147.94, 148.02, 150.78, 151.30, 151.33; FT-IR (KBr) *v*: 3398, 3066, 2938, 1637, 1608, 1566, 1535, 1475, 1423, 1381, 1279, 1213, 1070, 1036, 972, 807, 741 cm<sup>-1</sup>; ESI-MS *m/z*: 499.26 [M+H]<sup>+</sup>, 521.39 [M+Na]<sup>+</sup>; Anal. calcd for C<sub>30</sub>H<sub>22</sub>N<sub>6</sub>O<sub>2</sub>: C 72.28, H 4.45, N 16.86; found C 72.49, H 4.63, N 16.99.

### Acknowledgements

We are grateful to the financial supports from the Natural Science Foundation of Zhejiang province, China (Grant No. LY15B030006) and the National Natural Science Foundation of China (Grant No. 21103151).

### Supplementary data

Supplementary spectra related to this article can be found in the supporting information.

### References and notes

- [1] Xia, H.; Yang, J.; Fang, H. H.; Chen, Q. D.; Wang, H. Y.; Yu, X. Q.; Ma, Y. G.; Jiang, M. H.; Sun, H. B. *Chem. Phys. Chem.* **2010**, *11*, 1871–1875.
- [2] Fang, H. H.; Chen, Q. D.; Yang, J.; Wang, L.; Jiang, Y.; Xia, H.; Feng, J.; Ma, Y. G.; Wang, H. Y.; Sun, H. B. *Appl. Phys. Lett.* **2010**, *96*, 103508-1–103508-3.
- [3] Dahl, R.; Larsen, S.; Dohlmann, T. L.; Qvortrup, K.; Helge, J. W.; Dela, F.; Prats, C. *Acta Physiol.* **2015**, *213*, 145–155.
- [4] Verboven, P.; Herremans, E.; Helfen, L.; Ho, Q. T.; Abera, M.; Baumbach, T.; Wevers, M.; Nicolai, B. M. *Plant J.* **2015**, *81*, 169–182.
- [5] Lin, C. C.; Velusamy, M.; Chou, H. H.; Lin, J. T.; Chou, P. T. *Tetrahedron* **2010**, *66*, 8629–8634.
- [6] LaFratta, C. N.; Fourkas, J. T.; Baldacchini, T.; Farrer, R. A. *Angew. Chem. Int. Ed.* **2007**, *46*, 6238–6258.
- [7] Christenson, C. W.; Saini, A.; Valle, B. *J. Opt. Soc. Am. B* **2014**, *31*, 637–641 .
- [8] Li, L.; Wu, Y. Q.; Wang, Y. *Chin. Opt. Lett.* **2012**, *10*, 101602-1–101602-4.
- [9] Hu, D. Q.; Hu, Y. L.; Huang, W. H. *Opt. Commun.* **2012**, *285*, 4941–4945.
- [10] Sheng, N.; Liu, D. H.; Gu, B.; He, J.; Cui, Y. P. *Dyes. Pigm.* **2015**, *122*, 346–350.
- [11] Narayanan, S.; Abbas, A.; Raghunathan, S. P.; Sreekumar, K.; Kartha, C. S.; Joseph, R. *Rsc. Adv.* **2015**, *5*, 8657–8668.
- [12] Vanyukov, V.; Mikheev, G. M.; Mogileva, T. N.; Puzyr, A. P.; Bondar, V. S.; Svirko, Y. P. *Opt. Mater.* **2014**, *37*, 218–222 .
- [13] Zou, Q. L.; Zhao, H. Y.; Zhao, Y. X.; Fang, Y. Y.; Chen, D. F.; Ren, J. *J. Med. Chem.* **2015**, *58*, 7949–7958 .
- [14] Secret, E.; Maynadier, M.; Gallud, A.; Chaix, A.; Bouffard, E.; Gary-Bobo, M.; Marcotte, N.; Mongin, O.; Cheikh, K. E.; Hugues, V.; Auffan, M.; Frochot, C.; Morère, A.; Maillard, P.; Blanchard-Desce, M.; Sailor, M. J.; Garcia, M.; Durand, J. O.; Cunin, F. *Adv. Mater.* **2014**, *26*, 7643–7648.
- [15] Hamed, B.; Haimberger, T.; Kozich, V.; Wiehe, A.; Heyne, K. *Photochem. Photobiol.* **2014**, *295*, 53–56.
- [16] Reinhardt, B. A. *Chem. Mater.* **1998**, *10*, 1863–1874.

- [17] Albota, M.; Beljonne, D.; Bredas, J. L.; Ehrlich, J. E.; Fu, J. Y.; Heikal, A. A.; Hess, S. E.; Kogej, T.; Leven, M. D.; Marder, S. R.; McCord-Maughon, D.; Perry, J. W.; Röckel, H.; Rumi, M.; Subramaniam, G.; Webb, W. W.; Wu, X. L.; Xu, C. *Science* **1998**, *281*, 1653–1656.
- [18] Bhawalkar, J. D.; Shih, A.; Pan, S. J.; Liou, W. S.; Swiatkiewicz, J.; Reinhardt, B. A.; Prasad, P. N.; Cheng, P. C. *Bioimaging* **1996**, *4*, 168–178.
- [19] Yin, H. Y.; Xiao, H. B.; Ding, L.; Zhang, C.; Ren, A. M.; Li, B. *Mater. Chem. Phys.* **2015**, *151*, 181–186
- [20] He, T. C.; Too, P. C.; Chen, R.; Chiba, S.; Sun, H. D. *Chem. Asian J.* **2012**, *7*, 2090–2095.
- [21] Cao, D. X.; Liu, Z. Q.; Li, G. Z.; Liu, G. Q.; Zhang, G. H. *J. Mol. Struct.* **2008**, *874*, 46–50.
- [22] Hu, Z. J.; Sun, P. P.; Li, L.; Tian, Y. P.; Yang, J. X.; Wu, J. Y.; Zhou, H. P.; Tao, L. M.; Wang, C. K.; Li, M.; Chen, G. H.; Tang, H. H.; Tao, X. T.; Jiang, M. H. *Chem. Phys.* **2009**, *355*, 91–98.
- [23] Yi, X. Y.; Yang, P.; Huang, D. D.; Zhao, J. Z. *Dyes. Pigm.* **2013**, *96*, 104–115.
- [24] Zhang, X.; Li, L. L.; Liu, Y. K. *Mater. Sci. Eng. C* **2016**, *59*, 916–923.
- [25] Rigo, R.; Bianco, S.; Musetti, C.; Palumbo, M.; Sissi, C. *ChemMedChem* **2016**, *11*, 1762–1769.
- [26] Ali, S. S. *Org. Chem. Indian J.* **2011**, *7*, 270–274.
- [27] Zhang, H. G.; Tao, X. T.; Chen, K. S.; Yuan, C. X.; Jiang, M. H. *Synthetic Met.* **2011**, *161*, 354–359.
- [28] Gao, C.; Liu, S. Y.; Zhang, X.; Liu, Y. K.; Qiao, C. D.; Liu, Z. E. *Spectrochim. Acta, Part A* **2016**, *156*, 1–8.
- [29] Zhang, X.; Xie, R. X.; Yao, J. S.; Meng, X. L.; Liu, Y. K.; Yu, X. Q.; Jiang, M. H. *Polym. Polym. Compos.* **2012**, *20*, 9–12
- [30] Demas, J. N.; Crosby, G. A. *J. Phy. Chem.* **1971**, *75*, 991–1024.
- [31] Fromherz, P. *J. Phys. Chem.* **1995**, *99*, 7188–7192.
- [32] Narang, U.; Zhao, C. F.; Bhawalkar, J. D.; Bright, F. V.; Prasad, P. N. *J. Phys. Chem.* **1996**, *100*, 4521–4525.

- [33] Song, Q.; Evans, C. E.; Bohn, P. W. *J. Phys. Chem.* **1993**, *97*, 13736–13741.
- [34] Cao, X.; Tolbert, R.W.; McHale, J. L.; Edwards, W. D. *J. Phys. Chem. A* **1998**, *102*, 2739–2748.
- [35] Nad, S.; Kumbhakar, M.; Pal, H. *J. Phys. Chem. A* **2003**, *107*, 4808–4816.
- [36] Ren, Y.; Fang, Q.; Yu, W. T.; Lei, H.; Tian, Y. P.; Jiang, M. H. *J. Mater. Chem.* **2000**, *10*, 2025–2033.
- [37] Chandrasekhar, V.; Pandey, M. D.; Maurya, S. K.; Sen, P.; Goswami, D. *Chem. Asian J.* **2011**, *6*, 2246–2250.
- [38] Frisch, M. J.; Trucks, G. W.; Schlegel, H. B.; Scuseria, G. E.; Robb, M. A.; Cheeseman, J. R.; Zakrzewski, V. G.; Montgomery, J. A., Jr.; Stratmann, R. E.; Burant, J. C.; Dapprich, S.; Millam, J. M.; Daniels, A. D.; Kudin, K. N.; Strain, M. C.; Farkas, O.; Tomasi, J.; Barone, V.; Cossi, M.; Cammi, R.; Mennucci, B.; Pomelli, C.; Adamo, C.; Clifford, S.; Ochterski, J.; Petersson, G. A.; Ayala, P. Y.; Cui, Q.; Morokuma, K.; Malick, D. K.; Rabuck, A. D.; Raghavachari, K.; Foresman, J. B.; Cioslowski, J.; Ortiz, J. V.; Stefanov, B. B.; Liu, G.; Liashenko, A.; Piskorz, P.; Komaromi, I.; Gomperts, R.; Martin, R. L.; Fox, D. J.; Keith, T.; Al-Laham, M. A.; Peng, C. Y.; Nanayakkara, A.; Gonzalez, C.; Challacombe, M.; Gill, P. M. W.; Johnson, B. G.; Chen, W.; Wong, M. W.; Andres, J. L.; Head-Gordon, M.; Replogle, E. S.; Pople, J. A. *Gaussian 09*; Gaussian: Wallingford, CT, 2009.
- [39] (a) Hehre, W. J.; Ditchfield, R.; Pople, J. A. *J. Chem. Phys.* **1972**, *56*, 2257–2261; (b) Lee, C.; Yang, W.; Parr, R. G. *Rev. Phys. B* **1988**, *37*, 785–789; (c) Becke, A. D. *J. Chem. Phys.* **1993**, *98*, 5648–5652.
- [40] Albota, M. A.; Xu, C.; Webb, W.W. *Appl. Opt.* **1998**, *37*, 7352–7356.
- [41] (a) Imgartinger, H.; Herpich, R. *Eur. J. Org. Chem.* **1998**, *4*, 595–604; (b) Borisenko, K. B.; Zauer, K.; Hargittai, I. *J. Phys. Chem.* **1996**, *100*, 19303–19309.
- [42] Wendlandt, A. E.; Shannon, S. S. *J. Am. Chem. Soc.* **2014**, *136*, 506–512.
- [43] Nishizawa, T.; Lim, H. K.; Tajima, K.; Hashimoto, K. *J. Am. Chem. Soc.* **2009**, *131*, 2464–2465.

- [44] Soo, H. S.; Agiral, A.; Bachmeier, A.; Frei, H. *J. Am. Chem. Soc.* **2012**, *134*, 17104–17116.
- [45] Abbate, S.; Bazzini, C.; Caronna, T.; Fontana, F.; Gambarotti, C.; Gangemi, F.; Longhi, G.; Mele, A.; Sora, I. N.; Panzeri, W. *Tetrahedron* **2005**, *62*, 139–148.
- [46] Huang, Z. L.; Lei, H.; Li, N.; Qiu, Z. R.; Wang, H. Z.; Guo, J. D.; Luo, Y.; Zhong, Z. P.; Liu, X. F.; Zhou, Z. H. *J. Mater. Chem.* **2003**, *13*, 708–711.
- [47] Cai, Z. B.; Zhou, M.; Li, B.; Chen, Y.; Jin, F.; Huang, J. Q. *New J. Chem.* **2014**, *38*, 3042–3049.